Chronic airway fibrosis in orthotopic mouse lung transplantation models: an experimental reappraisal

Yamada, Yoshito ; Windirsch, Kevin ; Dubs, Linus ; Kenkel, David ; Jang, Jae-Hwi ; Inci, Ilhan ; Boss, Andreas ; Martinu, Tereza ; Vanaudenaerde, Bart M ; Weder, Walter ; Jungraithmayr, Wolfgang

Abstract: BACKGROUND: Several mouse lung transplantation (Tx) models have been proposed for the study of chronic airway fibrosis (CAF), the most prevalent complication seen in human lung transplant recipients, termed chronic lung allograft dysfunction (CLAD). Alternatively, it has been called for to establish an experimental animal model for restrictive allograft syndrome (RAS), another phenotype of CLAD. However, these mouse transplant models exhibit significant heterogeneity in consistency and reproducibility. We therefore aimed at reevaluating current available models. METHODS: 4 different Tx combinations were employed that manifest CAF: 2 minor antigen-mismatched Tx combinations (MINOR, donor: C57BL/10, recipient: C57BL/6J); or MINOR-N using recipient C57BL/6N, major histocompatibility antigen-mismatched immunosuppressed Tx (MAJOR, donor: BALB/c, recipient: C57BL/6J) and syngeneic Tx (SYN, donor and recipient: C57BL/6J) as control. The recipients were harvested and analyzed at week 8. Oxygenation, histology, reverse transcription polymerase chain reaction (RT-PCR), and magnetic resonance imaging were performed to analyze outcome of those models. RESULTS: The most prominent manifestation of CAF, thickest subepithelial fibrotic changes, worst oxygenation and the most severe acute rejection were detected in the MAJOR group, compared to all other ($p<0.05$). Gene expressions of TNF- and TGF- 1 were higher, and IL-10 was lower in the MAJOR group. Immunohistochemistry found pleuroparenchymal fibrotic change in both the MAJOR and MINOR-J group. CONCLUSIONS: We propose the major mismatch model under mild immunosuppression as the most suitable model for studying posttransplant CAF, and both the major and minor mismatch models for the restrictive phenotype.

DOI: https://doi.org/10.1097/TP.0000000000001917

Transplantation Publish Ahead of Print
DOI: 10.1097/TP.0000000000001917

Chronic Airway Fibrosis in Orthotopic Mouse Lung Transplantation Models – An Experimental Reappraisal

Yoshito Yamada, MD PhD[1], Kevin Windirsch, Msc[1], Linus Dubs Msc[1], David Kenkel, MD[2], Jae-Hwi Jang, PhD[1], Ilhan Inci, MD[1], Andreas Boss, MD PhD[2], Tereza Martinu, MD[3], Bart Vanaudenaerde, PhD[3], Walter Weder, MD[1], Wolfgang Jungraithmayr, MD PhD[1, 5*]

[1]Department of Thoracic Surgery, University Hospital Zurich, Zurich, Switzerland

[2]Institute of Diagnostic and Interventional Radiology at the University Hospital of Zurich, Switzerland

[3]University of Toronto, Ontario, Canada

[4]Laboratory of Pneumology, Katholieke Universiteit Leuven, Leuven, Belgium

[5]Department of Thoracic Surgery, Medical University Brandenburg, Campus Neuruppin, Germany

***Corresponding Author**

Wolfgang Jungraithmayr, MD PhD

Department of Thoracic Surgery

Medical University Brandenburg

Campus Ruppiner Kliniken

16816 Neuruppin

Germany

Telephone: +49 3391 394741

E-Mail (first): wolfgang.jungraithmayr@mhb-fontane.de

Email (second): wolfgang.jungraithmayr@usz.ch

Author's contributions

YY contributed to the experimental surgeries and retrieved and analyzed the data and codrafted the manuscript (MS); KK and LD analyzed the data; DK retrieved and analyzed the data; JJH contributed to the data analysis; II co-drafted the MS; AB contributed the data analysis and codrafted the MS; TM contributed the data analyses; WW codrafted the MS; WJ designed and coordinated the study and wrote the MS. All authors read and approved the final manuscript.

Disclosure

The authors declare no conflicts of interest.

Funding

None

Abbreviations

AR; acute rejection, BO; bronchiolitis obliterans, CAF; chronic airway fibrosis, CLAD; chronic lung allograft dysfunction, HE; hematoxylin and eosin, ISHLT; the international society for heart and lung transplantation, MAJOR; major histocompatibility antigen-mismatched, MINOR; minor histocompatibility antigen-mismatched, MRI; magnetic resonance imaging, MTR; magnetizing transfer ratio, RT-PCR; reverse transcription polymerase chain reaction, RF; radio frequency, αSMA, α smooth muscle actin; SYN; syngeneic, Tx; transplantation

Abstract

Background: Several mouse lung transplantation (Tx) models have been proposed for the study of chronic airway fibrosis (CAF), the most prevalent complication seen in human lung transplant recipients, termed chronic lung allograft dysfunction (CLAD). Alternatively, it has been called for to establish an experimental animal model for restrictive allograft syndrome (RAS), another phenotype of CLAD. However, these mouse transplant models exhibit significant heterogeneity in consistency and reproducibility. We therefore aimed at reevaluating current available models. ***Methods:*** 4 different Tx combinations were employed that manifest CAF: 2 minor antigen-mismatched Tx combinations (MINOR, donor: C57BL/10, recipient: C57BL/6J); or MINOR-N using recipient C57BL/6N, major histocompatibility antigen-mismatched immunosuppressed Tx (MAJOR, donor: BALB/c, recipient: C57BL/6J) and syngeneic Tx (SYN, donor and recipient: C57BL/6J) as control. The recipients were harvested and analyzed at week 8. Oxygenation, histology, reverse transcription polymerase chain reaction (RT-PCR), and magnetic resonance imaging were performed to analyze outcome of those models. ***Results:*** The most prominent manifestation of CAF, thickest subepithelial fibrotic changes, worst oxygenation and the most severe acute rejection were detected in the MAJOR group, compared to all other ($p<0.05$). Gene expressions of TNF-α and TGF-β1 were higher, and IL-10 was lower in the MAJOR group. Immunohistochemistry found pleuroparenchymal fibrotic change in both the MAJOR and MINOR-J group. ***Conclusions:*** We propose the major mismatch model under mild immunosuppression as the most suitable model for studying posttransplant CAF, and both the major and minor mismatch models for the restrictive phenotype.

Introduction

After decades of research, the phenomenon of chronic rejection in lung transplantation, clinically identified as chronic lung allograft dysfunction (CLAD), remains the most significant hurdle limiting long-term survival after lung transplantation (Tx). [1] CLAD affects 50% of cases by 5 years post-Tx, which is higher compared to chronic allograft rejection in other solid organ Tx, [1, 2] and the relative risk of death in CLAD patients compared to non-CLAD after lung Tx is more than 10 times higher. [3] CLAD comprises bronchiolitis obliterans syndrome (BOS) and/or restrictive allograft syndrome (RAS). [4, 5] Bronchiolitis obliterans (BO), a pathological aspect of BOS, is characterized by fibrous tissue deposits around and inside small airways, leading to airway constriction or obliteration. Alternatively, the histological characteristics of RAS is described as a temporal sequence of diffuse alveolar damage, followed by the development of pleuroparenchymal fibroelastosis. [4, 6] As chronic airway phenotypes in animal models are not identical to pathology of CLAD in clinical lung transplantation, we referred to pathological features of BO as 'intraluminal chronic airway fibrosis (intra-CAF)'. Alternatively, pathological features of RAS would be regarded as pleuroparenchymal, parenchymal or peribronchiolar fibrosis (peri-CAF).

In a light of these clinical issues, a robust and reproducible animal model that mimics the human condition is needed to discover effective treatment strategies. The establishment of the mouse model of lung Tx has pioneered scientific work due to its physiological nature when compared to the human setting, but also due to the availability of genetically engineered animals [7-9]. This mouse model has paved the way for the study of transplant-related phenomena and new

therapies. [7, 10] Using this model, 2 research groups were the first to propose new models in which lesions of airway fibrosis could be induced. [11, 12] The first experimental approach came from Fan and colleagues. [11] They employed a minor histocompatibility complex (MHC) mismatched mouse strain combination (C57BL/10 → C57BL/6N) to induce mild rejection and airway fibrosis that developed over the course of 4 weeks, with an airway obliteration rate of 44.4%. Shortly thereafter, the Leuven group proposed another approach using a fully MHC mismatched strain combination (BALB/c → C57BL/6) while mildly suppressing acute rejection with low-dose Cyclosporine and Methylprednisolone. [12] Several studies were done subsequently using 1 of these models. [13-15] About RAS development in mice, we could recently show that a fully MHC mismatched strain mouse lung Tx combination presented typical pathological features of RAS. [16]

We therefore aimed here at reevaluating and comparing the current available models in relation to the level of chronic airway fibrosis obtained at long-term and their ability to induce the restrictive phenotype.

Materials and Methods

Mice

Animals used in this study received care in strict accordance with the Principles of Laboratory Animal Care (National Institutes of Health Publication No. 85-23, promulgated in 1985, most recently revised in 1996). The local Veterinary Ethical Committee approved the study (study number 45/2014). Specific pathogen-free inbred male mice weighing 27 to 30 g were used for the study. Strain C57BL/6J ($H2^b$), C57BL/10J ($H\text{-}2^b$) and BALB/c ($H2^d$) were obtained from

Charles River Laboratories (Sulzfeld, Germany). C57BL/6N ($H2^b$) was purchased from Harlan Laboratories (Venray, The Netherlands).

Transplantation model and experimental groups

Orthotopic, left single-lung Tx was performed as described previously. [7, 17] The following experimental groups were formed (Table 1): (I) syngeneic (SYN) Tx between C57BL/6J mice (n=17); (II) Tx between minor mismatched mouse strains, deriving from Charles River laboratory (MINOR-J), C57BL/10J serving as donors and C57BL/6J serving as recipients (n=10); (III) Tx between minor mismatched mouse strains (MINOR-N), using C57BL/10J as donors and C57BL/6N as recipients (n=7); and (IV) Tx between major mismatched mouse strains (MAJOR), BALB/c serving as donors and C57BL/6J serving as recipients (n=12). We harvested and analyzed the recipients at 8 weeks to compare all the experimental groups, while we additionally harvested the samples in the MINOR-J Tx at 4 weeks (n=15) and at 12 weeks (n=7) to observe the kinetic change of this protocol. The rationale for testing both C57BL/6J and C57BL/6N, both substrains deriving from C57BL/6 and obtained from 2 different providers, is 2-fold: 1) The genetic drift that has led to disparate spontaneous mutations in C57BL/6J versus C57BL/6N mice may influence their susceptibility to airway fibrosis, [18] and 2) the provenance of animals may have an impact on phenotype expression due to environmental factors such as microbiome composition. [19] In the MAJOR group, daily doses of low-dose immunosuppressants were administered subcutaneously, including cyclosporine (10mg/kg/day) and methylprednisolone (1.6mg/kg/day), from the day of surgery to the day before harvest, based on previous studies. [12, 20]

Before graft explantation, arterial blood (200 µl) was aspirated from the descending aorta (without clamping the right hilum) for blood gas analysis. We considered mixed blood from the right and left lungs to be a reasonable representation of left lung dysfunction and hypoxia.

MRI and Magnetization transfer ratio

All datasets were acquired using a 4.7T PharmaScan (Bruker, Ettlingen, Germany). Mice were anesthetized during the acquisition of the datasets with isoflurane. Magnetization transfer ratio (MTR) is an MRI technique that can reveal characteristics of biotissue: The protons in water transfer the nuclear spin polarization from 1 population (free water) to another population (water "bound" to macromolecules). Using off-resonance radio frequency (RF) pulses, the RF energy is applied exclusively to the bound pool resulting in saturation of the macromolecular spins. Some of the spin saturation is then transferred to the free water pool. Thus, the free water pool becomes partially saturated leading to a reduction in the MRI signal compared to the acquisition without off-resonance pulse. This ratio between the signal reduction and the nonsaturated signal is called the Magnetization Transfer Ratio $MTR=(M_0-M_{sat})/M_0$. As magnetization transfer results in a reduction of the MRI signal, it is crucial that a MRI sequence is used which provides signal above the noise level, otherwise the reduction would not be measurable. Obtaining an MRI signal from lung tissue is nontrivial due to the ultrafast signal decay, which is caused by microscopic magnetic field inhomogeneities at tissue-air interfaces. We applied a zero echo-time sequence (ZTE) with radial k-space readout capable to detect lung signal. The ZTE sequence was equipped with an off-resonance prepulse with adaptable off-resonance frequency and flip angle. After acquisition of the data with nominal prepulse flip angle of 1000 or 3000° and off-resonance frequencies of 1000, 2000, 3000, 4000, 6000, 8000, 10000 and 15000Hz, MTR values were calculated and

compared, and MTR maps were depicted with in-house computer programs. [21, 22]

Histology and Immunhistochemistry

Tx lungs from each group were fixed in 4% phosphate-buffered formalin, cut, and embedded in paraffin. Sections of 4-μm thickness were cut and stained with hematoxylin and eosin (HE) stain, Masson's Trichrome stain and Elastica van Gieson stain. For the histological evaluation, the pathological severity of acute rejection (AR) and CAF were assessed by 3 different investigators. AR grading (A-grade) was based on the guidelines of the international society for heart and lung transplantation (ISHLT). [23] We defined chronic airway fibrosis (CAF) as eosinophilic hyaline fibrosis in the submucosa of membranous and respiratory bronchioles (peri-CAF) or intraluminal fibrosis of the airways (intra-CAF). [23] We evaluated each graft for the presence of absence of any airways obliterated (completely or partially) with intraluminal fibrosis. In addition, we scored the degree of fibrotic changes in peri-CAF, intra-CAF and pleuroparenchymal fibrosis, grading on a general scale of 0-4.

For morphometric analysis, we applied a quantitative assessment of airway wall thickness so that only peribronchiolar fibrotic lesions could be objectively evaluated. The volume fraction of subepithelial connective tissue was measured from the basement membrane to the outer edge of the airway adventitia (Vv_{sub}) by the public domain image processing program ImageJ. Airway wall thickness was calculated by dividing Vv_{sub} by the length of the subepithelial basement membrane. [15, 24, 25] We randomly chose 5 bronchioles with distinguishable structure and the diameter of 150 μm in each left graft.

Immunohistochemistry was performed as previously described. [17] Primary antibodies

were mouse anti smooth muscle actin (αSMA) mAb (1A4, Dako Denmark A/S, Glostrup, Denmark) and rabbit anti vimentin mAb (D21H3, BioConcept, Allschwil, Switzerland), rabbit anti-CD3 mAb (RMAB005, Diagnostic Biosystems, Pleasanton, CA), rat anti F4/80 mAb (T-1006, BMA Biomedicals, Augst, Switzerland), rat anti B220 mAb (RA3-6B2, BD Biosciences Europe, Allschwil, Switzerland) and goat anti NKp46 Ab (NCR1, BD Biosciences Europe, Allschwil, Switzerland). Mouse spleen was used for positive control with the primary antibodies, while samples without primary antibody served as negative control. We assessed each sample grading on a general scale of 0-4.

Quantitative real-time PCR

Total RNA was extracted by mirVana Paris kit (Ambion, Thermo Fisher Scientific, Waltham, MA) following the manufacturer's instructions. Five micrograms of RNA were used for reverse transcription by ThermoScript reverse transcription polymerase chain reaction (RT-PCR) System (Invitrogen, Thermo Fisher Scientific) yielding cDNA template. Quantitative real-time PCR amplification and data analysis were performed using 7500 Fast Real-Time PCR System (Applied Biosystems, Thermo Fisher Scientific). Taq Man gene expression assays were used to quantify mRNA expression of the respective genes. mRNA expression levels of each sample were normalized to 18S RNA (Taq Man rRNA control reagents; Applied Biosystems, Thermo Fisher Scientific). All mRNA expression data was calculated as fold change from naïve animal tissues.

Statistics

Histological evaluations as ordinal variables were depicted in scatter plots, showing the median value. In comparisons of ordinal variables among the groups, Kruskal-Wallis test was used; in continuous variables, analysis of variance with a post hoc Tukey test was performed; and in categorical variables Fischer's exact test with Bonferroni's correction was applied to determine differences. A 2-sided p value < 0.05 was considered statistically significant. Prism 5 (GraphPad Software Inc., La Jolla, CA) was used for the statistical calculations.

Results

Development of airway fibrotic lesions varied between models

Control syngeneic transplants showed neither lymphocytic infiltration nor fibrotic changes (Figure 1A, B, Figure 2A, B). Transplanted lungs in the MINOR-J group showed moderate perivascular and peribronchiolar inflammation with periairway fibrosis (Figure 1C, D; Figure 2C, D). Grafts in the MINOR-N group showed the same degree of inflammation as the MINOR-J (Figure 1E, F; Figure 2E, F). In contrast, allografts in the MAJOR group presented severe lymphocytic infiltration in perivascular and peribronchiolar areas, mostly graded as A4 (Figure 1G, H), paralleled by accumulation of fibrotic tissue around and inside airways, as well as the parenchyma (Figure 2G, H). The evaluation of the pathological score of AR based on the ISHLT guidelines [23] revealed that MAJOR had distribution with higher AR scores compared to other groups (Figure 1G, H; Figure 3) ($p<0.05$). AR scores between MINOR-J and MINOR-N were comparable (Figure 1. C-F; Figure 3). SYN showed relatively lower AR scores than others, although there were no significant differences (Figure 1A, B; Figure 3).

Table 1 gives the overview of intra-CAF in all samples. Ten out of 12 (83%) of grafts in MAJOR showed obliterated airway, while none in either MINOR-J or MINOR-N at every time point, yielding statistical significant differences between MAJOR and others ($p<0.0033$ with Bonferroni's correction). Likewise, the scoring evaluation with 8-week graft for intra-CAF showed the significant differences between MAJOR and others by Kruskal-Wallis test ($p<0.05$) (Figure 4A). About peri-CAF, both MAJOR and MINOR-J showed distributions with higher fibrotic change score, compared to SYN ($p<0.05$). MAJOR also presented significant difference compared to MINOR-N (Figure 4B). We also examined pleural and parenchymal fibrotic changes in the same manner for CAF evaluation. In pleural evaluation, MINOR-J and MAJOR showed comparable fibrotic degrees, but both were higher than the SYN (Figure S1A, SDC, http://links.lww.com/TP/B474). In parenchymal fibrosis, the MAJOR group showed relatively higher than MINOR-J, although no significant difference (Figure S1B, SDC, http://links.lww.com/TP/B474).

We also examined immunohistochemistry on 8 week grafts to elucidate what kind of cells were involved. In the evaluation of extra cellular matrix, MAJOR showed significantly higher grades in αSMA than other groups (Figure 5A, C, E, G, Figure 6). Also in vimentin, MAJOR had higher scores than SYN and MINOR-J. The intensity of immune cells such as T cells, B cells, macrophages and NK cells were comparable between MINOR-J and MAJOR, while SYN presented the lower intensity on that immunohistochemistry compared to the 2 groups. (Figure S2, S3, SDC, http://links.lww.com/TP/B474).

Morphometric analysis detected prominent peri-CAF in the MAJOR group

A morphometric analysis of grafts was performed to calculate the airway wall thickness for an objective evaluation of peribronchiolar fibrosis. MAJOR showed significantly thickest airway walls of all, while SYN showed thinnest airway walls (Figure 7, $p<0.05$).

Decreased oxygenation in immunosuppressed major mismatch mice (MAJOR group)

For the investigation of the functionality of transplant lungs, blood gas analysis was performed. 200 μl of arterial blood was withdrawn at the 8th week from the abdominal aorta of recipients. The MAJOR group presented significantly lower levels of PaO_2/FiO_2 than others ($p<0.05$) (Figure 8).

TNF-α and TGF-β1 were elevated in MAJOR

We analyzed levels of inflammatory and antiinflammatory cytokines within recipient transplants in the grafts of the MINOR-J group and the MAJOR group by RT-PCR (Figure 9). Gene expression levels of the Th1 cytokine TNF-α was significantly elevated in the MAJOR group compared to the MINOR, while levels of the Th2 cytokine IL-10 was lower than the MINOR group. Additionally, levels of TGF-β1, which plays a pivotal role in the development of fibrosis, were elevated in the MAJOR group.

MR imaging detects CAF

We next evaluated whether a novel MR imaging technology has the potential for the detection and evaluation of the extension of CAF. Typical examples are provided in Figure 10. In overall, MTR values on left grafts was higher than naïve right lungs, while infiltrated lung without

CAF exhibited higher MTR values compared to infiltrated lungs with CAF for all frequencies and flip angles (data not shown).

Discussion

In this study, we reevaluated the currently available mouse lung transplant models of CAF. We combined different strains and protocols in order to identify the most consistent model. We found that the combination of major mismatched Tx (MAJOR) revealed the highest rate of intraluminal airway fibrosis, which developed in 83% of grafts 8 weeks after lung Tx, and the most severe periairway fibrosis. Additionally, both the minor and major mismatched Tx presented pathological features of RAS phenotype.

The finding that a minor mismatched strain combination develops CAF has been a pioneering finding by Fan, Wilkes and colleagues. [11] This Tx combination induces a low-grade but continued development of allograft rejection with a mild degree of immune cell infiltration over time which does not completely damage the transplanted graft as it is known from the major BALB/c → C57BL/6 combination. [17] Several groups have used this minor mismatched strain model in their studies. [13-15] The development of airway obliteration in these studies was between 0% and 44%, at 3 to 4 weeks after Tx. [14] The exact cause of such variability in this model remains unclear. In our hands, however, using the similar mouse strains with C57BL/6J did not show any airway obliteration. This variation may be due to strain variability and environmental factors between substrains and animal providers. [14] The use of 2 different providers in prior studies, namely C57BL/6N and C57BL/6J, prompted us to include the C57BL/6N for testing of this hypothesis. However, this strain did not develop airway obliteration either. Alternatively,

Chang et al, showed that allografts with warm ischemia in a minor mismatch combination in rat lung transplant presented higher ratio of occluded airway compared to allografts only with cold ischemia. [26] Likewise, Watanabe et al, presented that the minor combination only with cold ischemia did not develop BO pathology at all, but some allografts in this combination added with warm ischemia. [27] In order to induce chronic airway fibrosis in the minor combination, a certain degree of damage such as warm ischemia might be necessary. Along with this context, a report from Mimura et al, is of higher interest: employing a B6D2F1/J strain (a cross breeding between C57BL/6J and DBA/2J, H2b/d) for the donor and a DBA/2J strain (H2d) for the recipient, the development ratio of airway obliteration was 100%. [15] This showed another evidence that allodifference of the minor combination was just not enough to induce chronic airway fibrosis. To rule out that allografts of the minor combination developed obliteration changes, we monitored them by harvesting on 4 weeks, 8 weeks and 12 However, there was no morphological change.

In human lung transplantation, allorecognition and MHC mismatching may not fully account for development of CAF lesions. Many factors are thought to play a role in a complex clinical setting. Nonimmunological injuries such as viral or bacterial infections, primary graft dysfunction (innate immunity) and acid aspiration by the patient contribute to the complex picture of CLAD and obliterative bronchiolitis. Also, self-antigens seem to play a role in the genesis of CLAD. In this context, the group from Mohanakumar and colleagues introduced a model where mice were given intratracheal administrations of antibodies against self-antigens such as type V Collagen (Col-V) or K-alpha-1-tubulin, which already have shown to play important roles in acute or chronic rejection [28]. However, although this model revealed 80% lesions of peri-CAF, the lack of an actual lung transplant makes it a little more different from the clinical scenario.

In our studies, we have shown a higher prevalence and severity of CAF in the fully major histocompatibility complex mismatched combination with low-dose immunosuppression [12]. The 2 advantages of this model are that this protocol simulates the clinical setting of allotransplantation across a major MHC mismatch with the induction of AR, and the concomitant application of immunosuppression. The mechanism of CAF development in this model seems to be more complex and multifactorial as it is found in human Tx. Indeed, when reproducing this protocol, it resulted in 83% of the development of airway obliterate lesions 8 weeks after Tx. On the other hand, as a disadvantage, this protocol takes longer to generate the fully developed obliterated airway lesions. Although in our hands, the MAJOR group confirmed to be the most reliable and consistent model of CAF, the logistic effort to develop lesions is quite high in terms of long-term daily administration of immunosuppressant.

Both MINOR-J and MINOR-N showed thicker airway walls and higher peri-CAF scores compared to SYN. Moreover, the evaluation for pleural fibrosis presented comparable fibrotic scores among MINOR-J, MINOR-N and MAJOR, all significantly higher than SYN. These pathological findings were suggestive for RAS development [3, 4, 6] We reported before that the MAJOR combination using immunosuppression revealed RAS pathology. [16] The current study showed that not only the major mismatched combination but also the minor combination might present pathological features of RAS, suggesting these protocols as experimental models to investigate RAS phenotype of CLAD. Indeed, some experimental studies already employed peribronchial fibrosis as an end-point to discuss CLAD. [28-30]

Cytokine analyses reflected the development of CAF among the experimental groups. Recent evidence suggests that Th1 and Th17 influence CLAD after lung transplantation. [31] While TGF-β is essential in Th17 differentiation, this cytokine itself also plays a pivotal role in the development of fibrosis. [32] Our cytokine analyses corroborate previous findings showing that the MAJOR group had prominent CAF with elevated gene levels of Th1 cytokines and TGF-β1. We furthermore observed comparable expressions of T cells, B cells, macrophages and NK cells between the Minor and the Major combination, although those phenotypes are relevant during CLAD development. [14, 33-36] Antigens of the extracellular matrix such as vimentin, Col V and K-alpha-1-tubulin are key factors for CLAD development. [37, 38] We speculated that these factors could be the most decisive for BO phenotype of CLAD.

We previously suggest MR imaging for the detection of acute rejection. [39] Higher protein content in the infiltrated lung tissue leading to significantly higher magnetization transfer due to the interaction of macromolecular spin pool with the water spin pool is thought to be the mechanisms behind. We here could observe differences of MTR values between allograft with and without CAF. This was prosumably due to interaction of collagen and the “free-water-protons”, particularly when sufficiently high off-resonance frequencies were chosen in order to preclude relevant direct saturation effects. We believe from these data that MRI could be a putative tool to detect CAF after lung transplantation.

Taken together, among the most recent and relevant experimental CLAD models proposed, the major histocompatibility mismatched combination treated by low-dose immunosuppression seems to be the most consistent model with highest yields of CAF in our hands. This model reflects most closely the clinical situation thus making it an appealing tool for finding new therapeutics against CLAD in lung Tx. However, for an even more complete model, viral and bacterial infections as well as nonimmunological injuries to the transplant could be added to make a CLAD model even more relevant for a transfer of findings and knowledge into clinical application.

Acknowledgment

The authors thank Christine Opelz, Pia Fuchs and Ursula Suess for their valuable technical help.

References

1. Yusen RD, Edwards LB, Kucheryavaya AY, et al. The Registry of the International Society for Heart and Lung Transplantation: thirty-second official adult lung and heart-lung transplantation report--2015; focus theme: early graft failure. *J Heart Lung Transplant*. 2015;34(10):1264-1277.
2. Suhling H, Gottlieb J, Bara C, et al. Chronic rejection: differences and similarities in various solid organ transplants. *Internist (Berl)*. 2016;57(1):25-37.
3. Sato M, Ohmori-Matsuda K, Saito T, et al. Time-dependent changes in the risk of death in pure bronchiolitis obliterans syndrome (BOS). *J Heart Lung Transplant*. 2013;32(5):484-491.
4. Verleden GM, Raghu G, Meyer KC, et al. A new classification system for chronic lung allograft dysfunction. *J Heart Lung Transplant*. 2014;33(2):127-133.
5. Royer PJ, Olivera-Botello G, Koutsokera A, et al. Chronic lung allograft dysfunction: a systematic review of mechanisms. *Transplantation*. 2016;100(9):1803-1814.
6. Ofek E, Sato M, Saito T, et al. Restrictive allograft syndrome post lung transplantation is characterized by pleuroparenchymal fibroelastosis. *Mod Pathol*. 2013;26(3):350-356.
7. Jungraithmayr WM, Korom S, Hillinger S, Weder W. A mouse model of orthotopic, single-lung transplantation. *J Thorac Cardiovasc Surg*. 2009;137(2):486-491.
8. Jungraithmayr W, Weder W. The technique of orthotopic mouse lung transplantation as a movie-improved learning by visualization. *Am J Transplant*. 2012;12(6):1624-1626.

9. Yamamoto S, Yamane M, Yoshida O, et al. Early growth response-1 plays an important role in ischemia-reperfusion injury in lung transplants by regulating polymorphonuclear neutrophil infiltration. *Transplantation*. 2015;99(11):2285-2293.
10. Okazaki M, Krupnick AS, Kornfeld CG, et al. A mouse model of orthotopic vascularized aerated lung transplantation. *Am J Transplant*. 2007;7(6):1672-1679.
11. Fan L, Benson HL, Vittal R, et al. Neutralizing IL-17 prevents obliterative bronchiolitis in murine orthotopic lung transplantation. *Am J Transplant*. 2011;11(5):911-922.
12. De Vleeschauwer S, Jungraithmayr W, Wauters S, et al. Chronic rejection pathology after orthotopic lung transplantation in mice: the development of a murine BOS model and its drawbacks. *PLoS One*. 2012;7(1):e29802.
13. Hirayama S, Sato M, Loisel-Meyer S, et al. Lentivirus IL-10 gene therapy down-regulates IL-17 and attenuates mouse orthotopic lung allograft rejection. *Am J Transplant*. 2013;13(6):1586-1593.
14. Wu Q, Gupta PK, Suzuki H, et al. CD4 T cells but not Th17 cells are required for mouse lung transplant obliterative bronchiolitis. *Am J Transplant*. 2015;15(7):1793-1804.
15. Mimura T, Walker N, Aoki Y, et al. Local origin of mesenchymal cells in a murine orthotopic lung transplantation model of bronchiolitis obliterans. *Am J Pathol*. 2015;185(6):1564-1574.
16. Yamada Y, Vandermeulen E, Heigl T, et al. The role of recipient derived interleukin-17A in a murine orthotopic lung transplant model of restrictive chronic lung allograft dysfunction. *Transpl Immunol*. 2016;39:10-17.

17. Yamada Y, Jang JH, De Meester I, et al. CD26 costimulatory blockade improves lung allograft rejection and is associated with enhanced interleukin-10 expression. *J Heart Lung Transplant*. 2016;35:508-517.
18. Simon MM, Greenaway S, White JK, et al. A comparative phenotypic and genomic analysis of C57BL/6J and C57BL/6N mouse strains. *Genome Biol*. 2013;14(7):R82.
19. Reliene R, Schiestl RH. Differences in animal housing facilities and diet may affect study outcomes-a plea for inclusion of such information in publications. *DNA Repair (Amst)*. 2006;5(6):651-653.
20. Vessie EL, Hirsch GM, Lee TD. Aortic allograft vasculopathy is mediated by CD8(+) T cells in Cyclosporin A immunosuppressed mice. *Transpl Immunol*. 2005;15(1):35-44.
21. Wurnig MC, Weiger M, Wu M, et al. In vivo magnetization transfer imaging of the lung using a zero echo time sequence at 4.7 Tesla in mice: initial experience. *Magn Reson Med*. 2015;76(1):156-162.
22. Kenkel D, Yamada Y, Weiger M, et al. Magnetization transfer as a potential tool for the early detection of acute graft rejection after lung transplantation in mice. *J Magn Reson Imaging*. 2015;44(5):1091-1098.
23. Stewart S, Fishbein MC, Snell GI, et al. Revision of the 1996 working formulation for the standardization of nomenclature in the diagnosis of lung rejection. *J Heart Lung Transplant*. 2007;26(12):1229-1242.
24. Hogg JC, Chu F, Utokaparch S, et al. The nature of small-airway obstruction in chronic obstructive pulmonary disease. *N Engl J Med*. 2004;350(26):2645-2653.

25. Polosukhin VV, Cates JM, Lawson WE, et al. Bronchial secretory immunoglobulin a deficiency correlates with airway inflammation and progression of chronic obstructive pulmonary disease. *Am J Respir Crit Care Med*. 2011;184(3):317-327.
26. Chang JC, Leung JH, Tang T, et al. In the face of chronic aspiration, prolonged ischemic time exacerbates obliterative bronchiolitis in rat pulmonary allografts. *Am J Transplant*. 2012;12(11):2930-2937.
27. Watanabe T, Martinu T, Oishi H, et al. Ischemia reperfusion injury augments acute and chronic rejection and alloimmune-dependent intrapulmonary lymphoid neogenesis in a mouse orthotopic lung transplant model. *J Heart Lung Transplant*. 2017;36(4):191-192.
28. Subramanian V, Ramachandran S, Banan B, et al. Immune response to tissue-restricted self-antigens induces airway inflammation and fibrosis following murine lung transplantation. *Am J Transplant*. 2014;14(10):2359-2366.
29. Martinu T, Gowdy KM, Nugent JL, et al. Role of C-C motif ligand 2 and C-C motif receptor 2 in murine pulmonary graft-versus-host disease after lipopolysaccharide inhalations. *Am J Respir Cell Mol Biol*. 2014;51(6):810-821.
30. Martinu T, Kinnier CV, Sun J, et al. Allogeneic splenocyte transfer and lipopolysaccharide inhalations induce differential T cell expansion and lung injury: a novel model of pulmonary graft-versus-host disease. *PLoS One*. 2014;9(5):e97951.
31. Gracon AS, Wilkes DS. Lung transplantation: chronic allograft dysfunction and establishing immune tolerance. *Hum Immunol*. 2014;75(8):887-894.

32. Xu Z, Ramachandran S, Gunasekaran M, et al. MicroRNA-144 dysregulates the transforming growth factor-beta signaling cascade and contributes to the development of bronchiolitis obliterans syndrome after human lung transplantation. *J Heart Lung Transplant*. 2015;34(9):1154-1162.
33. Xu Z, Ramachandran S, Gunasekaran M, et al. B cell-activating transcription factor plays a critical role in the pathogenesis of anti-major histocompatibility complex-induced obliterative airway disease. *Am J Transplant*. 2016;16(4):1173-1182.
34. Takenaka M, Tiriveedhi V, Subramanian V, et al. Antibodies to MHC class II molecules induce autoimmunity: critical role for macrophages in the immunopathogenesis of obliterative airway disease. *PLoS One*. 2012;7(8):e42370.
35. Fildes JE, Yonan N, Tunstall K, et al. Natural killer cells in peripheral blood and lung tissue are associated with chronic rejection after lung transplantation. *J Heart Lung Transplant*. 2008;27(2):203-207.
36. Jungraithmayr W, Codarri L, Bouchaud G, et al. Cytokine complex-expanded natural killer cells improve allogeneic lung transplant function via depletion of donor dendritic cells. *Am J Respir Crit Care Med*. 2013;187(12):1349-1359.
37. Yamada Y, Sekine Y, Yoshida S et al. Type V collagen-induced oral tolerance plus low-dose cyclosporine prevents rejection of MHC class I and II incompatible lung allografts. J Immunol 2009; 183: 237-245.
38. Sullivan JA, Jankowska-Gan E, Hegde S, et al. Th17 responses to collagen type V, kalpha1-Tubulin, and vimentin are present early in human development and persist throughout life. *Am J Transplant*. 2017;17(4):944-956.

39. Kenkel D, Yamada Y, Weiger M, et al. Magnetization transfer as a potential tool for the early detection of acute graft rejection after lung transplantation in mice. *J Magn Reson Imaging*. 2016;44(5):1091-1098.

Figure legends

Figure 1: Representative H&E histology of lung grafts on the 8th week in lower magnification (25x: A, C, E, G) and higher magnification (100x: B, D, F, H). Grafts of a syngeneic combination (SYN) showed no lymphocytic infiltration (A0) (A, B). Grafts of minor histocompatibility antigen mismatched combination with C57BL/6J (MINOR-J) showed moderate infiltration (C, D) as well as the MINOR-N with C57BL/6N (E, F). Grafts of major histocompatibility antigen mismatched combination (MAJOR) had severe lymphocytic infiltration and intraluminal fibrotic changes with airway obliteration (G, H). Scale bars indicates 500 μm on A, C, E and G, and 200 μm on B, D, F and H. MAJOR; major histocompatibility antigen mismatched combination, MINOR; minor histocompatibility antigen mismatched combination, SYN; syngeneic combination.

Figure 2: Representative Trichrome staining histology of lung grafts corresponding to Figure 1 (25x: A, C, E, G; 100x: B, D, F, H). Grafts of the SYN group showed no fibrosis (A, B). Grafts of MINOR-J and -N presented mild fibrotic changes in peribronchiolar areas (C, D, E, F). Grafts of MAJOR showed not only peribronchiolar fibrosis but also intraluminal fibrotic airway obliteration (G, H). Scale bars indicates 500 μm on A, C, E and G, and 200 μm on B, D, F and H. MAJOR; major histocompatibility antigen mismatched combination, MINOR; minor histocompatibility antigen mismatched combination, MT; Masson's Trichrome staining, SYN; syngeneic combination.

Figure 3: Scatter plots of acute rejection scores of 8 week grafts based on the ISHLT guidelines. AR scores of the MAJOR group were distributed in higher grades, and Kruskal-Wallis test detected significant differences in comparisons of MAJOR to SYN, MINOR-J or MINOR-N ($p<0.05$). Bars indicate medians of values. An asterisk indicates significant difference. MAJOR; major histocompatibility antigen mismatched combination, MINOR; minor antigen mismatched combination, SYN; syngeneic combination.

Figure 4: Scatter plots of fibrotic evaluation of 8 week grafts in intraluminal area (intra-CAF) and peribronchiolar areas (peri-CAF) graded with 0-4 score. (A) Only the MAJOR group had allografts (10/12) with intra-CAF distributing from score 1 to 3, instead other groups have none. Kruskal-Wallis test detected significant differences between MARJOR and others ($p<0.05$). (B) Both MAJOR and MINOR-J showed distributions with higher fibrotic change score in peri-CAF, compared to SYN ($p<0.05$). MAJOR also presented significant difference compared to MINOR-N. Bars indicate median of values. Asterisks indicate significant difference. CAF; chronic airway fibrosis, MAJOR; major histocompatibility antigen mismatched combination, MINOR; minor histocompatibility antigen mismatched combination, SYN; syngeneic combination.

Figure 5: Representative immunohistochemistry for αSMA (25x: A, C, E, G) and Vimentin (25x: B, D, G, H) of 8 week grafts. The MAJOR group showed higher intensity of the positive cells on each staining than others. Scale bars indicates 500 μm. MAJOR; major histocompatibility antigen mismatched combination, MINOR; minor histocompatibility antigen mismatched combination, SYN; syngeneic combination.

Figure 6: The intensity of positive cells in αSMA and Vimentin immunohistochemistry (Figure 1) graded with 0-4 scores. (A) The MAJOR group presented distribution with higher scores in αSMA immunohistochemistry, showing significant differences compared to other groups ($p<0.05$). (B) MAJOR presented distribution with higher scores in Vimentin immunohistochemistry, yielding significant differences compared to SYN or MINOR-J ($p<0.05$). Bars indicate medians of values. Asterisks indicate significant differences. MAJOR; major histocompatibility antigen mismatched combination, MINOR; minor histocompatibility antigen mismatched combination, SYN; syngeneic combination.

Figure 7: Peribronchiolar airway wall thickness. Airway thickness was compared among groups. MAJOR showed significantly thickest airway walls of all (‡, $p<0.05$); while SYN was the thinnest of all (†, $p<0.05$). Error bars show standard deviations. MAJOR; major histocompatibility antigen mismatched combination, MINOR; minor histocompatibility antigen mismatched combination, SYN; syngeneic combination.

Figure 8: Blood gas analysis on week 8. PaO2/FiO2 ratios in the MAJOR group were significantly lowest ($p<0.05$). The asterisk indicates the significant differences compared to other groups. Error bars show standard deviations. MAJOR; major histocompatibility antigen mismatched combination, MINOR; minor histocompatibility antigen mismatched combination, SYN; syngeneic combination.

Figure 9: Cytokine analyses by RT-PCR. MAJOR presented higher levels of TNF-α (A) and TGF- β1 (C) and lower levels of IL-10 (B), compared to MINOR-J. Error bars show standard deviations. Asterisks indicate significant differences. MAJOR; major histocompatibility antigen mismatched combination, MINOR; minor histocompatibility antigen mismatched combination; RT-PCR; reverse transcription polymerase chain reaction.

Figure 10: MRI images and MTR maps. Recipient mice with and without CAF on the 8th week were examined by MRI depicting ananatomical map (A, C) and magnetizing transfer ratio (MTR) map with a flip angle of 1000° and an off-resonance frequency of 3000 Hz (B, D). The dotted areas indicate transplanted grafts. In each group, the MTR intensity on the left graft was higher than the naïve right lung. On the other hand, the MTR intensity on the graft in 'CAF (-)' was higher than 'CAF (+)'. CAF; chronic airway fibrosis, MTR; magnetizing transfer ratio

Figure 1

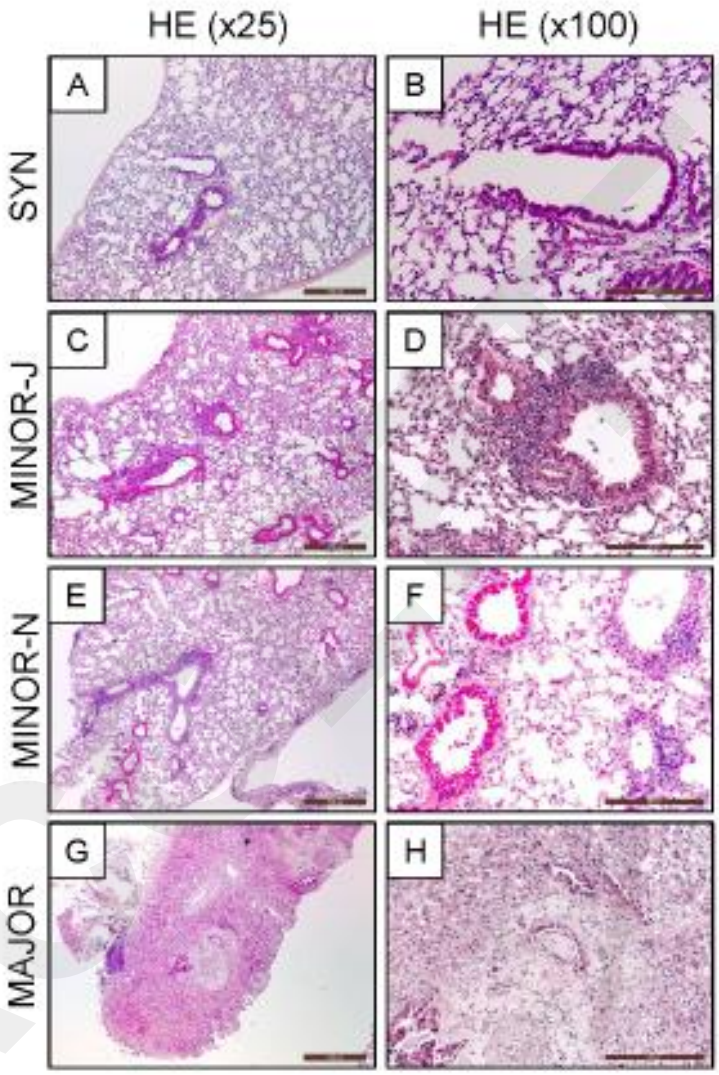

Figure 2

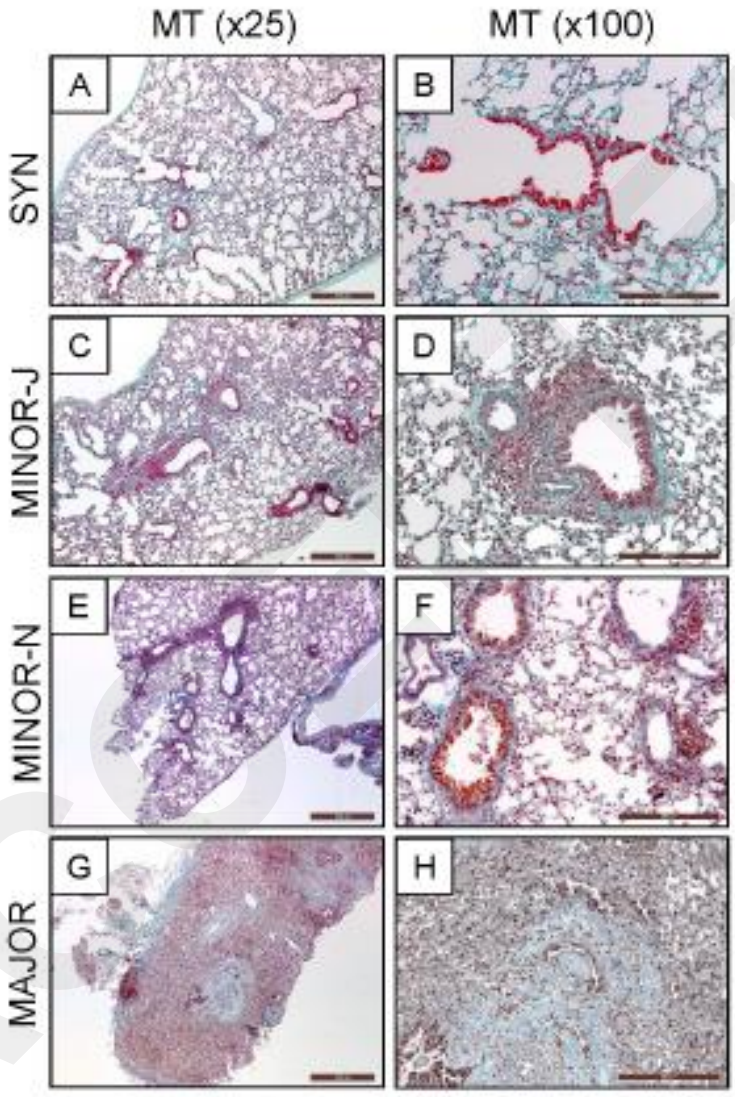

Figure 3

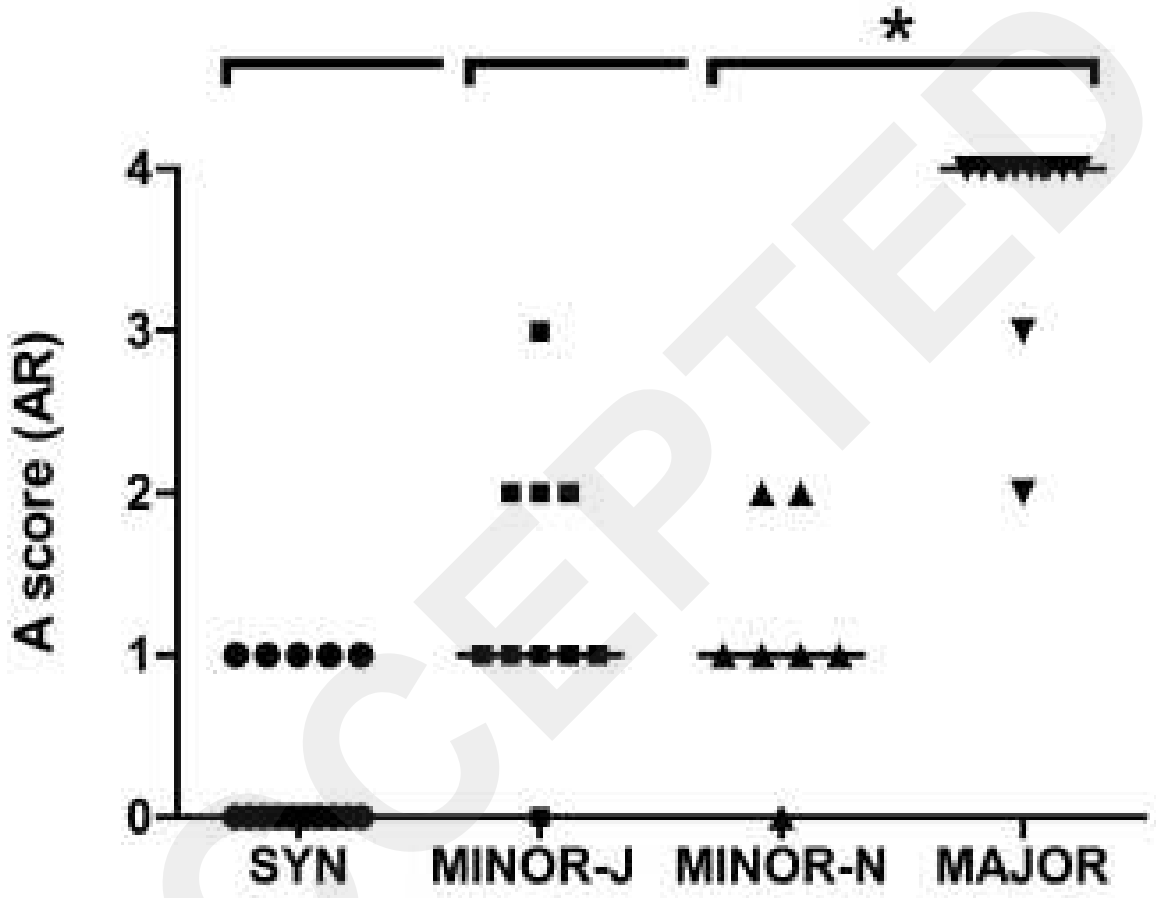

Figure 4

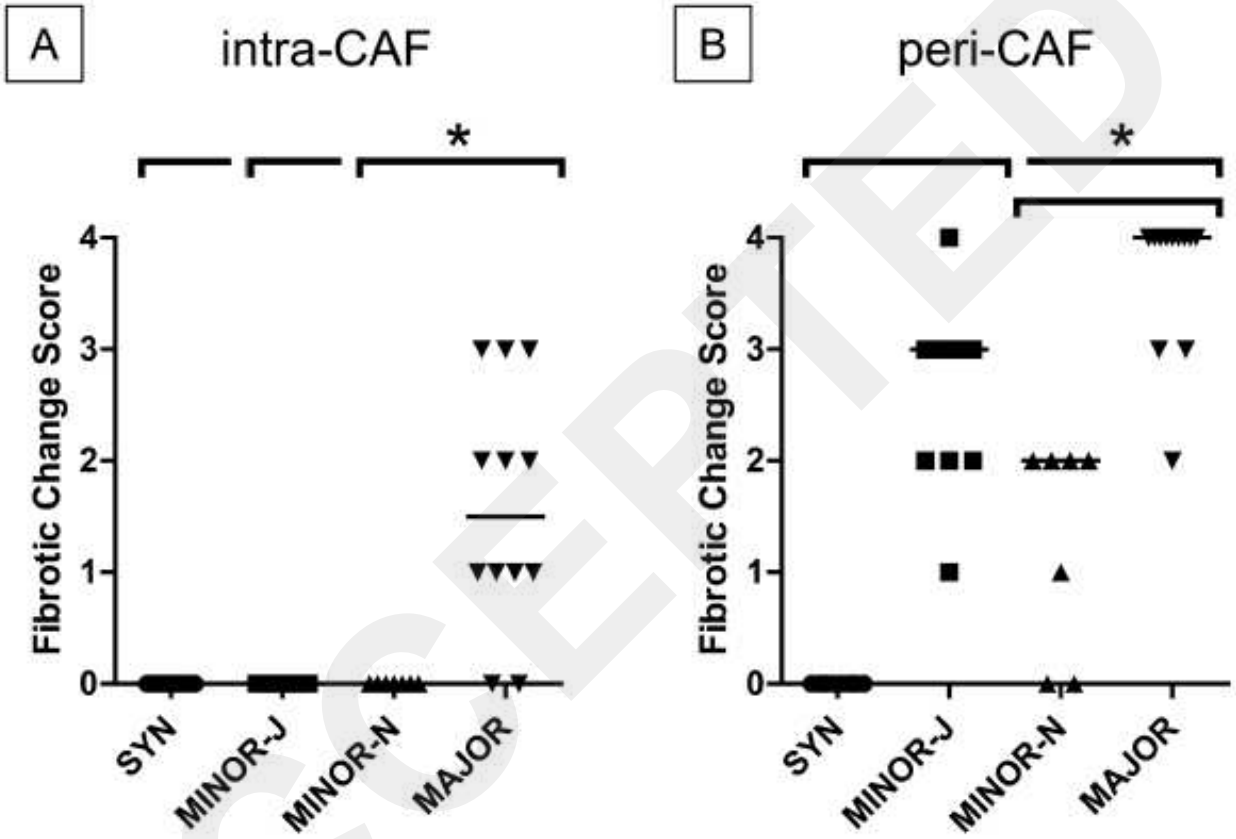

Figure 5

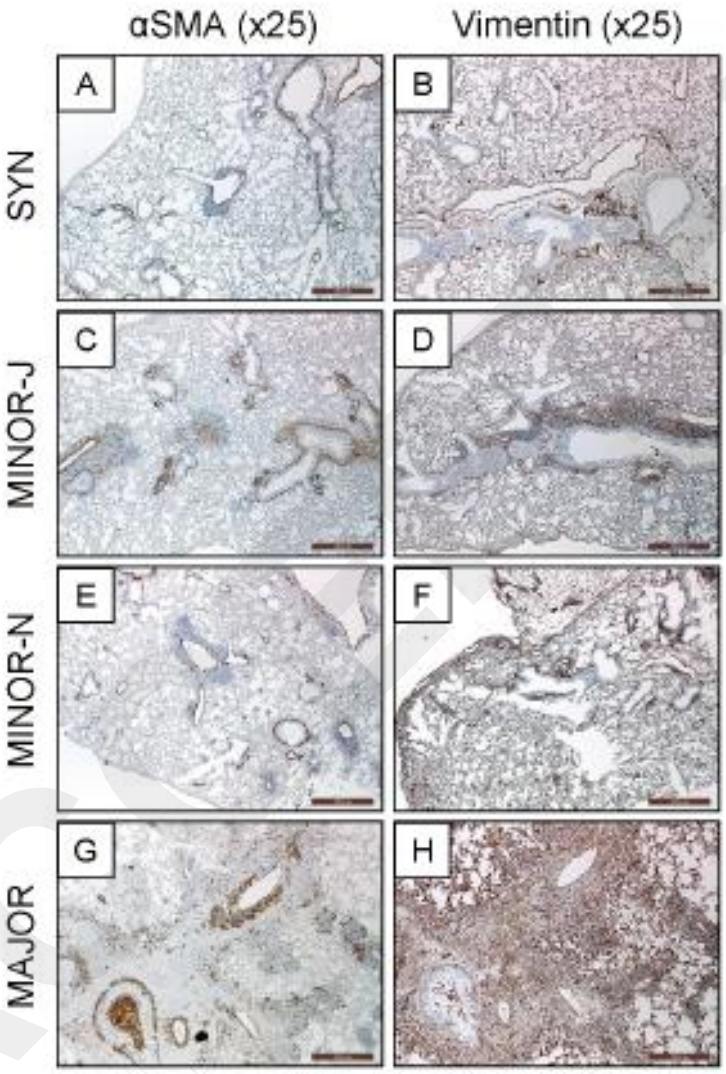

Figure 6

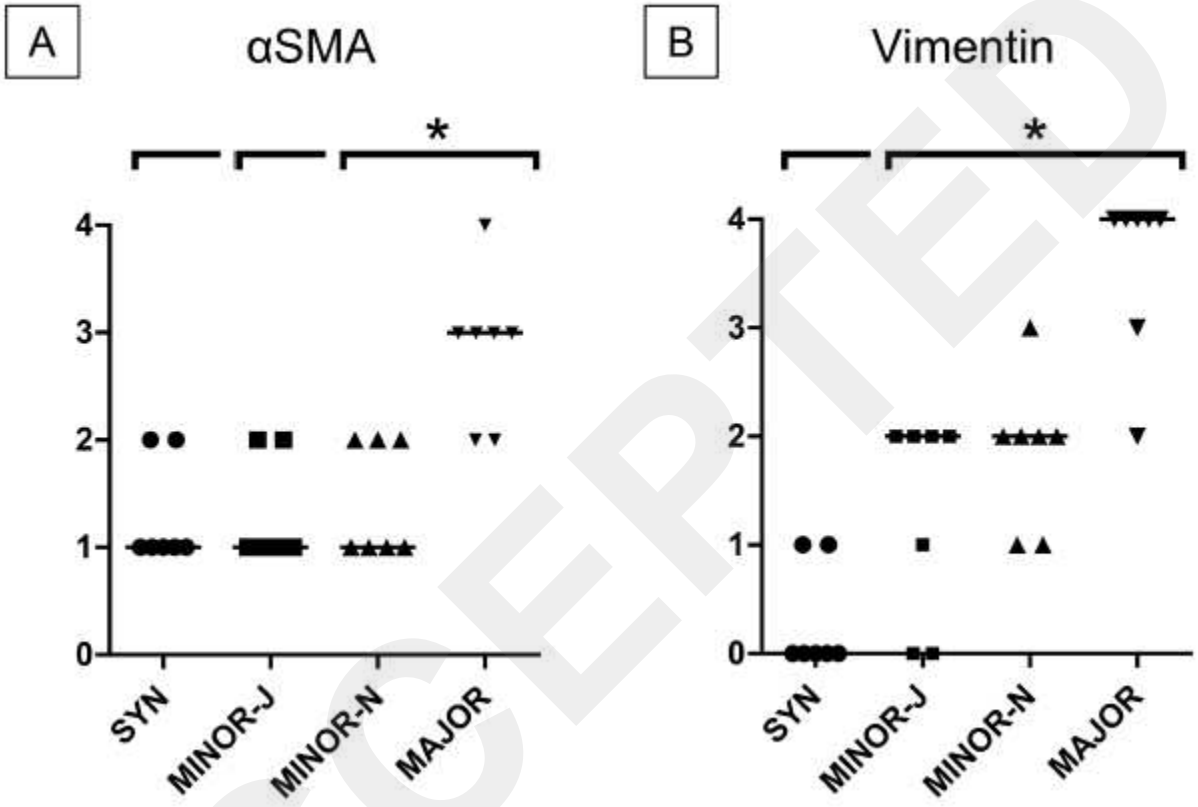

Figure 7

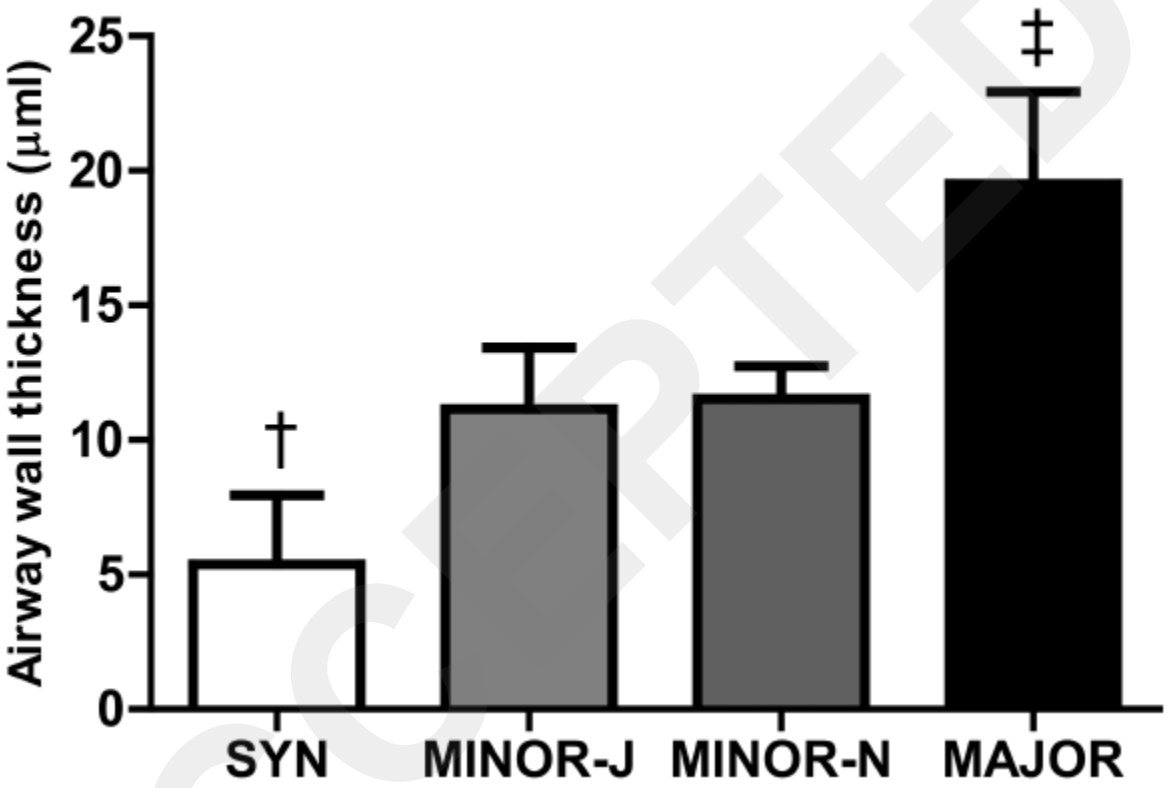

Figure 8

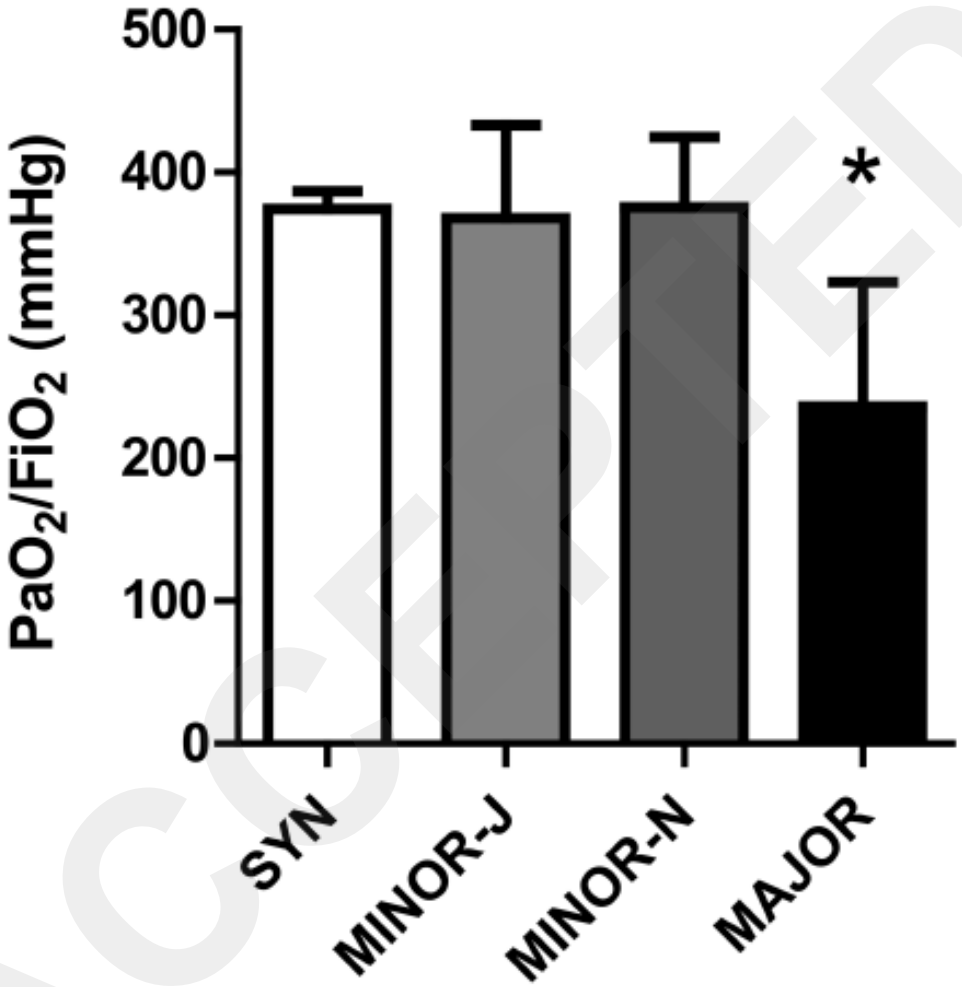

Figure 9

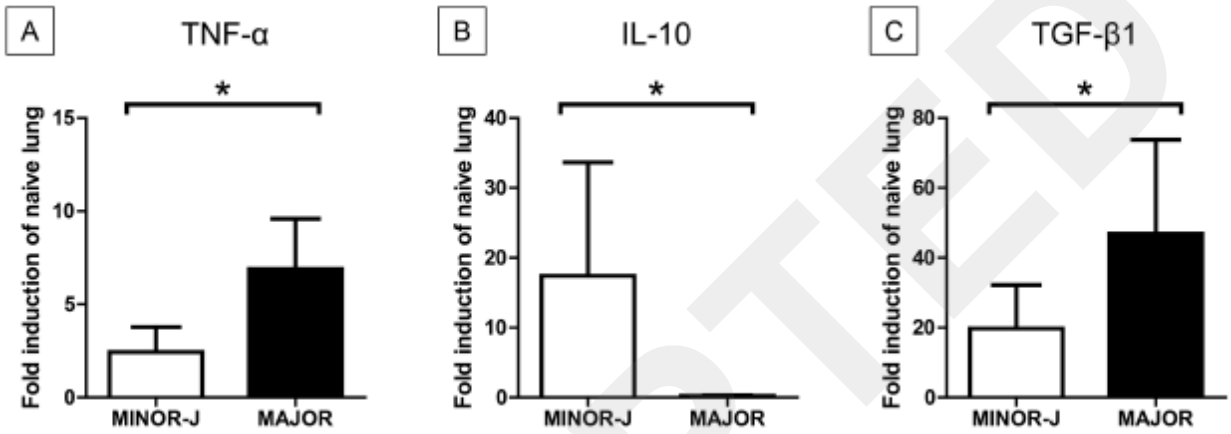

Figure 10

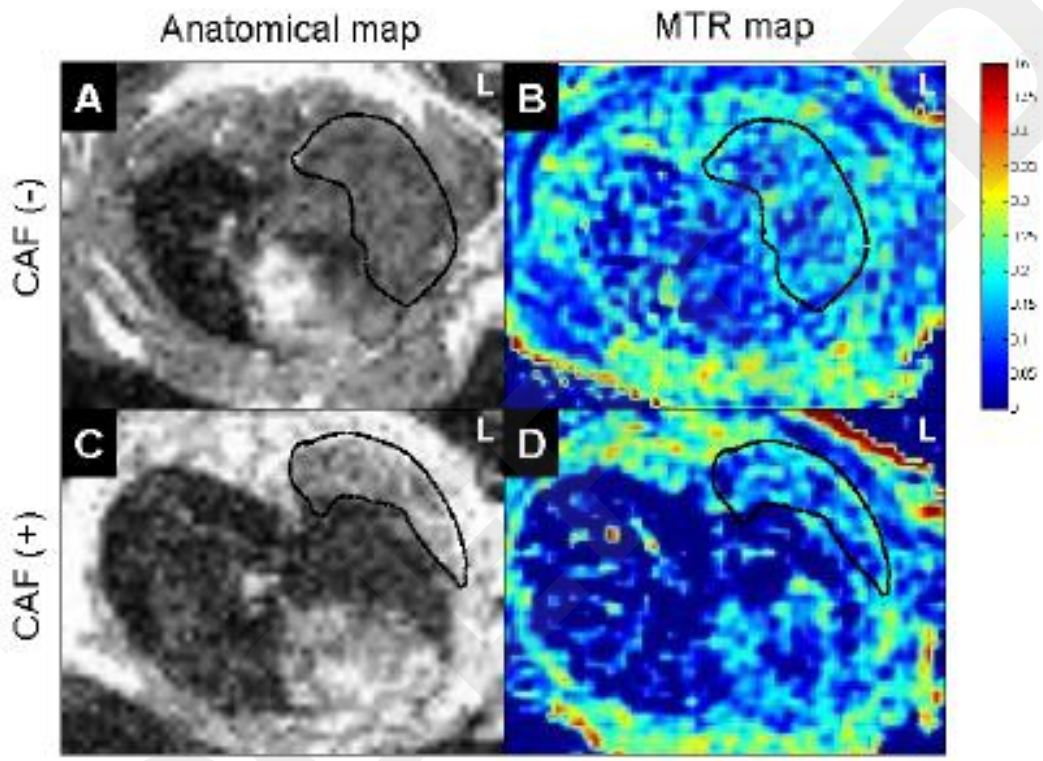

Table 1: List of the experimental groups and the development of intra-CAF

Experimental group	SYN	MINOR-J	MINOR-N	MAJOR
Donor	C57BL/6J	C57BL/10J	C57BL/10J	BALB/c
Recipient	C57BL/6J	C57BL/6J	C57BL/6N	C57BL/6J
Immunosuppressant	No	No	No	Yes
intra-CAF/ Total mice (%)				
4 weeks after Tx	-	0/ 15 (0) *	-	-
8 weeks after Tx	0/17 (0) *	0/ 10 (0) *	0/ 7 (0) *	10/12 (83.3)
12 weeks after Tx	-	0/ 7 (0) *	-	-

* Significant difference compared with the MAJOR group harvested on the 8th week ($p<0.05$).

intra-CAF; intraluminal chronic airway fibrosis, MAJOR; major histocompatibility antigen mismatched combination, MINNOR; minor histocompatibility antigen mismatched combination, SYN; syngeneic combination, Tx; transplantation

Supplemental Figure 1: Evaluation for pleural and parenchymal fibrosis. Fibrotic changes in pleura or parenchyma of grafts on week 8 were graded with 0-4 score. (A) MINOR-J, MINOR-N and MAJOR showed comparable pleural fibrotic changes, which presented distributions with higher grades compared to SYN. (B) In parenchymal fibrosis, differences between SYN and MAJOR were observed. Bars indicate medians of values. Asterisks indicate significant differences. MAJOR; major histocompatibility antigen mismatched combination, MINOR; minor histocompatibility antigen mismatched combination, SYN; syngeneic combination.

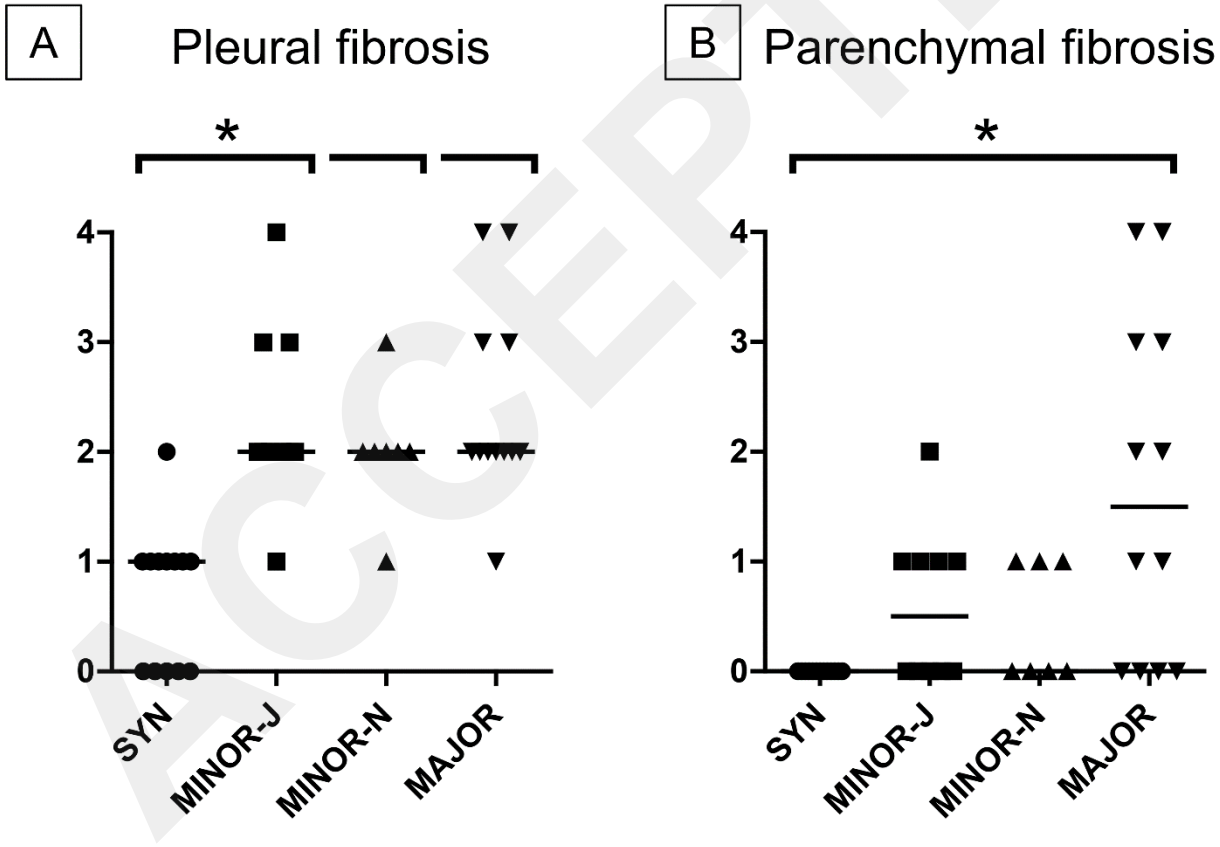

Supplemental Figure 2: Representative immunohistochemistry of CD3 (T cell, 25x: A, E, I), B220 (B cell: 25x: B, F, J), F4/80 (macrophage: 100x: C, G, K) and NKp46 (NK cell: 100x: D, H, L) of 8 week grafts. Scale bars indicates either 500 µm (A, B, E, F, I, J) or 200 µm (C, D, G, H, K, L). MAJOR; major histocompatibility antigen mismatched combination, MINOR; minor histocompatibility antigen mismatched combination, SYN; syngeneic combination.

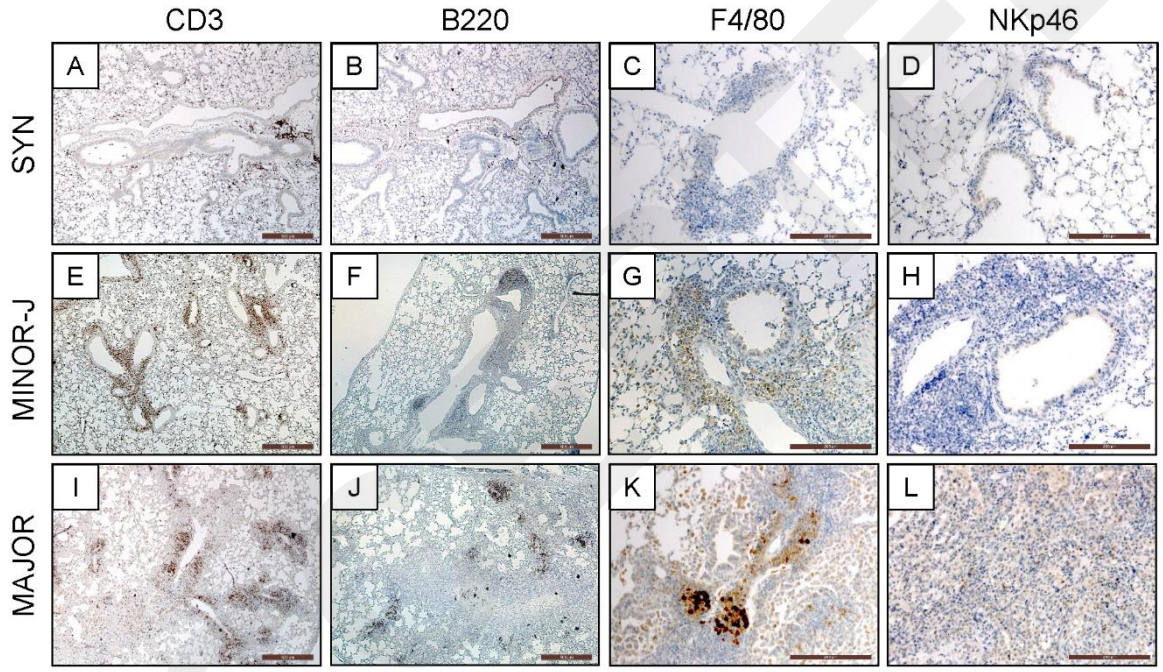

Supplemental Figure 3: Analyses of the intensity of positive cells in the immunohistochemistry on the supplemental Figure 2. Both MINOR-J and MAJOR presented distributions of CD3 (A), B220 (B) and F4/80 (C) with higher intensity compared to SYN ($p<0.05$). The intensities in NKp46 were comparable among the groups. Bars indicate medians of values. Asterisks indicate significant differences. MAJOR; major histocompatibility antigen mismatched combination, MINOR; minor histocompatibility antigen mismatched combination, SYN; syngeneic combination.